Nanoscale Advances

ROYAL SOCIETY OF CHEMISTRY

REVIEW

View Article Online
View Journal | View Issue

Check for updates

Cite this: *Nanoscale Adv.*, 2025, **7**, 4551

Electron spin resonance with scanning tunneling microscopy: a tool for an on-surface quantum platform of identical qubits

Deung-Jang Choi, *[abc] Soo-hyon Phark, [de] Andreas J. Heinrich [de] and Nicolás Lorente [ab]

Integration of electron spin resonance (ESR) in a scanning tunneling microscope (STM) has enabled all-electrical control of atomic and molecular spins on solid surfaces with atomic-scale precision and energy resolution beyond thermal limitations. Further, coherent manipulation and detection of individual spins in an ESR-STM establishes a powerful quantum platform, allowing for the implementation of fundamental quantum logic operations to on-surface identical qubits (same chemical species but ESR-adressable). In this review, we introduce recent advances of ESR-STM, focusing on its application to atomic-scale qubits and extension to molecular qubit systems. We discuss the principles underlying ESR-STM, followed by single-spin addressability, coherent control *via* Rabi oscillations, and quantum state readout through frequency-resolved detection. We further demonstrate multi-qubit control architectures enabled by atom manipulation and local magnetic field engineering, culminating in the realization of multi-qubit logic gates such as the Controlled-NOT and Toffoli gates. These implementations highlight the specialty of ESR-STM towards atomic-scale quantum circuits. Indeed, ESR-STM can be an excellent tool to perform and evaluate quantum operations in molecular qubits. The results reviewed in this collection establish ESR-STM as a versatile tool for advancing quantum coherent science at the atomic and molecular level in solid-state environments.

Received 4th April 2025
Accepted 20th June 2025

DOI: 10.1039/d5na00316d

rsc.li/nanoscale-advances

Open Access Article. Published on 10 July 2025. Downloaded on 12/3/2025 1:48:05 AM.
This article is licensed under a Creative Commons Attribution 3.0 Unported Licence.

1. Introduction

Quantum computing represents a paradigm shift in our computational capabilities, offering the potential to solve problems that remain intractable for classical architectures.[1] At its core, quantum computing exploits qubits—quantum analogs of classical bits that can exist in coherent superpositions—to process information in parallel. Various platforms have been explored for qubit realization, ranging from superconducting circuits[2] and trapped atoms[3] to semiconductor quantum dots.[4] Despite noteworthy progress in coherence time and gate fidelity, challenges such as the complexity of cryogenic electronics[5] and fabrication limits persist.

Electron spin resonance (ESR)[6] offers the high energy resolution required for precise spin measurements, independent of thermal broadening, while scanning tunneling microscopy (STM) provides atomic-scale spatial resolution.[7] The synergistic combination of these techniques in an ESR-STM thus enables addressing of individual spins with energy resolutions reaching tens of neV in the study of single atoms, atomically controlled structures, and molecules.[8–13] Construction and coherent control of nanoscale qubit systems are central to advancing quantum-coherent nanoscience.[14] In this regard, coherent manipulation of single electron spins *via* radio-frequency (RF) excitation in an ESR-STM[15,16] have marked a milestone in the bottom-up approach to construct qubit architectures utilizing individual atoms on a solid surface. However, achieving the full potential of this approach necessitates scaling beyond the confines of a subnanometer junction to incorporate multiple, addressable qubits.[17]

In this context, molecular spins emerge as an attractive alternative to conventional two-level systems. Their rich internal structures not only allow for the possibility of multi-level quantum computation but also provide a versatile platform for tailoring energy level architectures that facilitate robust quantum error correction protocols.[18–20] Moreover, the natural propensity of molecules to self-assemble offers a pathway far more efficient than atoms in fabricating high-density qubit arrays—a crucial attribute for scalable quantum computing architectures.[21–23] The atomic-scale spatial resolution and high energy discrimination inherent to ESR-STM are

[a]*Centro de Física de Materiales CFM/MPC (CSIC-UPV/EHU), 20018 Donostia-San Sebastián, Spain. E-mail: djchoi@dipc.org*
[b]*Donostia International Physics Center (DIPC), 20018 Donostia-San Sebastián, Spain*
[c]*Ikerbasque, Basque Foundation for Science, 48013 Bilbao, Spain*
[d]*Center for Quantum Nanoscience (QNS), Institute for Basic Science (IBS), Seoul 03760, Republic of Korea*
[e]*Department of Physics, Ewha Womans University, Seoul 03760, Republic of Korea*

© 2025 The Author(s). Published by the Royal Society of Chemistry

Open Access Article. Published on 10 July 2025. Downloaded on 12/3/2025 1:48:05 AM. This article is licensed under a Creative Commons Attribution 3.0 Unported Licence.

therefore ideally suited for investigating and controlling the complex quantum states in molecular systems.[24,25]

This article reviews the unique capabilities of ESR-STM to achieve quantum-coherent manipulation of both atomic[17] and molecular[26] qubits. By harnessing the full quantum state space offered by these systems, we seek to overcome current scalability limitations and pave the way for the realization of high-density, robust quantum computing platforms.

2. ESR-STM

Coherent control of individual qubits is fundamental to any quantum computation scheme. ESR-STM represents a powerful approach for such control at the atomic and molecular scale.[14–16] In 2015, ESR in an STM was first demonstrated for electron spins localized in single atoms on a surface using a continuous-wave (CW) RF signal.[8] The next major step forward was the demonstration of pulsed driving of ESR in 2019, which enabled quantum state manipulation of electron spin in a titanium (Ti) atom (Fig. 1).[15]

In ESR-STM, spin manipulation is achieved by applying a RF modulated bias voltage to the tunnel junction formed between an STM tip and a spin center adsorbed on a substrate. The RF bias induces transitions in the quantum states of the spin when the radio frequency matches the Larmor frequency of the spin, resulting in a detectable change in tunneling current.[8] This allows for a precise measurement of spin resonance with an energy resolution down to some tens of neV, far exceeding the limit due to thermal broadening. Moreover, by applying RF pulses of controlled duration and amplitude, it is possible to induce coherent rotations of the spin. The phase, frequency, duration and amplitude of the driving pulse determine the quantum state evolution of the spin, enabling a full control of the corresponding qubit vector on the Bloch sphere.[15,27,28]

Fig. 1 presents a schematic diagram of the ESR-STM setup, used in the first demonstration on coherent control of single atomic spins on a surface.[15] The system combines the STM's capability of spatially addressing individual atoms or molecules with driving of ESR in a time-controlled manner, allowing for coherent control of electron spins of single Ti adsorbates on a 2-monolayer-thick (2 mL) MgO decoupling layer prepared on an Ag(100) substrate.[15,27,28] In a simplified scheme, the spin-polarized (SP) tip apex plays a crucial role for ESR experiments in an STM in terms of both driving and probing the magnetic resonance of the spin in the tunneling junction: (i) in general, time-dependent Hamiltonian matrix elements $\langle 1|H\Lambda_1(t)|0\rangle$ are required for transitions between the two states $|0\rangle$ and $|1\rangle$ of the electron spin[29–31] that will depend on the relative angle between the spins of tip and atom for the ESR excitation. Besides, due to this angle, the flowing electrons can cause a torque on the atomic spin, leading to spin pumping effect in the target atom. (ii) In analogy to a model of magnetic tunnel junction, first the SP-tip can be seen as one magnetic electrode. Second, together with the spin-polarization of the target atom, it induces a tunneling magneto-resistance effect. When driving ESR of the atom, this magneto-resistance changes from that of the non-driven state, resulting in a corresponding change in the tunneling current, which is the readout of ESR-STM. In addition, when the spins of the tip and atom are not collinear, the precessing components of the atomic spin perpendicular to the quantization axis can couple to the phase of the V_{RF}, leading to the homodyne contribution to the detected signal.

For pulsed-ESR, the RF-signal output is modulated by an arbitrary waveform generator to create RF-pulses with well-

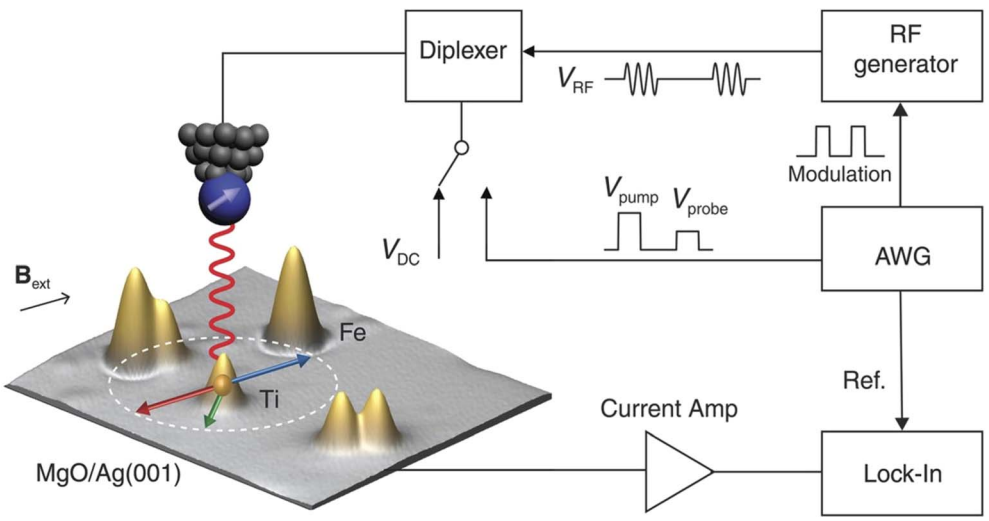


Fig. 1 Scheme of a scanning tunneling microscope prepared for performing pulsed ESR experiments on single atoms such as Ti on a MgO/Ag(100) substrate. The STM tip is shown above a surface with several atomic or molecular structures (possible impurities or nanostructures). A radio-frequency (RF) voltage is added *via* a diplexer on the DC bias of the STM. The introduction of an arbitrary waveform generator (AWG) in the radio frequency generation leads to the creation of control pulses with a time resolution of 1 ns and sub-milliVolt amplitudes. Adapted from (ref. 15).

© 2025 The Author(s). Published by the Royal Society of Chemistry

Open Access Article. Published on 10 July 2025. Downloaded on 12/3/2025 1:48:05 AM. This article is licensed under a Creative Commons Attribution 3.0 Unported Licence.

controlled width and amplitudes. This RF pulse, controlled at a nanosecond time scale, drives a fraction of rotation of the target spin within its coherence time, which enables coherent control experiments such as Rabi oscillation, Ramsey fringe, spin-echo, and so on, as demonstrated first by K. Yang *et al.* in 2019.[15]

3. ESR-STM as a quantum platform

To evaluate the potential of ESR-STM beyond laboratory demonstration, we outline below the essential requirements, current capabilities, and open challenges for deploying ESR-STM as a viable quantum platform.

3.1. Requirements for ESR-STM-compatible quantum systems

To be suitable for quantum information applications using ESR-STM, a quantum system must fulfill several stringent conditions: (i) atomic-scale stability on cryogenic surfaces, (ii) discrete and well-isolated spin states with controllable anisotropy, (iii) compatibility with microwave frequency excitation at the tunnel junction, and (iv) efficient spin-sensitive tunneling for readout. These conditions are typically met by carefully selected magnetic adatoms on ultrathin insulating films grown on metallic substrates.[14,15] As we showed in the previous section, MgO/Ag (100) is well suited substrate for ESR-STM of single atomic spins for the last decade. In addition, there are reports of ESR signals on other substrates, such as Terbium bisphthalocyanato on NaCl/Cu(100).[32]

3.2. Current capabilities and performance metrics

Recent experiments have demonstrated coherent control of single-spin qubits on surfaces using ESR-STM. Using this technique the typical values characterizing the spin evolution are spin-relaxation times T_1 up to microseconds in selected atomic systems; quantum coherence times $T_2 \sim 200$ ns, measured *via* spin-echo sequences;[15] 1-qubit operations based on Rabi and Ramsey sequences and two-axis universal control has been demonstrated using phase-controlled RF pulses;[17] readout is performed through ESR-induced modulation of the tunneling current; this typically requires signal averaging and limits single-shot readout fidelity. Despite this promising values, gate fidelities remain to be systematically benchmarked. We will explore in detail the present status of quantum gates with the ESR-STM in the following section.

Compared to other atomic-scale platforms, ESR-STM offers unique advantages such as a sub-Å spatial resolution, direct control of inter-qubit coupling *via* tip-induced potentials, and the possibility of engineering artificial spin structures atom by atom. However, unlike platforms based on color centers or trapped ions, ESR-STM still lacks intrinsic optical initialization and scalable photonic integration.[14]

3.3. Challenges for scalability and quantum computing

Scaling ESR-STM to multi-qubit quantum information platforms involves substantial experimental and technological challenges. Some of these challenges are the surface and material degradation. Over time, atomically engineered spin structures may suffer from tip-induced drift, surface contamination, or atomic rearrangement, affecting stability and coherence.

Another problem inherent of STM-based techniques is the tip reproducibility and conditioning. Indeed, spin-polarization and magnetic stability of a SP-tip have been known to be hard to control due to its strong dependence on the microscopic structure of the magnetic tip apex as well as working conditions, leading to varying magnetic orders and field-responses.[33–35] Therefore, the spin-polarized and RF-sensitive tips required for ESR-STM are challenging to prepare and often irreproducible, complicating parallelization. In this regard, special attention needs to be granted to local environment control, because small variations in the electrostatic environment, work function, or film thickness can significantly alter the spin Hamiltonian, reducing reproducibility. STM is an inherently serial technique. Multiplexed control and scalable readout will require new paradigms in microwave delivery, nanoplasmonic enhancement, or on-chip resonator integration.

An important aspect is the one related to identical qubits (same chemical species but ESR-adressable). Achieving arrays of identical qubits implies uniform local environments, homogeneous magnetic anisotropy, and precise control over exchange couplings—conditions that are hard to maintain over extended arrays. On the other hand, qubit architectures made of same-species atoms are virtually identical except for small variations of the environment. Using local probes like the tip itself or local magnetic nanostructures (a nearby Fe atom),[27] the local field can be used to shift the properties of the qubit and make it addressable among many virtually-identical qubits.

While ESR-STM remains a laboratory-intensive technique, it offers compelling advantages for bottom-up quantum control at the atomic scale. The recent demonstration of universal qubit rotations[28] marks a key milestone towards quantum gate implementations. Addressing the outlined challenges will be essential for advancing ESR-STM from single-spin spectroscopy towards a viable quantum simulation or computation platform.[14,15]

4. Quantum gates in ESR-STM

Driving ESR of qubits creates a unitary evolution of the qubits, the so called quantum gates. By controlling the time duration of the driving pulse, the evolution can be terminated to leave the qubit in a predetermined quantum state along a Rabi oscillation. By applying a sequence of pulses, furthermore, different unitary evolutions are chained together, leading to a complex coherent manipulation of the qubit state.

4.1. Single-qubit gate

A series of RF pulses tuned to the Larmor frequency of a single atom spin can produce desired single-qubit quantum gates in ESR-STM. A simple example is the Hadamard gate as illustrated in Fig. 2(a) using the Bloch sphere and vector representation.

Open Access Article. Published on 10 July 2025. Downloaded on 12/3/2025 1:48:05 AM.
This article is licensed under a Creative Commons Attribution 3.0 Unported Licence.

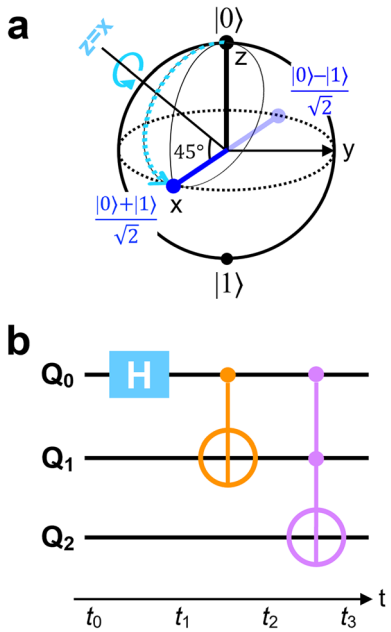


Fig. 2 (a) A scheme using the Bloch sphere illustrating Hadamard gate to a qubit initialized to its $|0\rangle$ state. (b) A quantum circuit to generate a maximally-entangled Greenberger–Horne–Zeilinger (GHZ) state when all three qubits (Q_0, Q_1, Q_2) are initialize to $|0\rangle$ states. The circuit implements a Toffoli (Controlled-Controlled-NOT; CCNOT) gate, the third gate (purple), which flips the state of the third qubit, Q_2 if and only if the other two qubits are in the state $|1\rangle$. The first gate (cyan), Hadamard gate (H), creates a superposition state $(|0\rangle + |1\rangle)/\sqrt{2}$ of Q_0. The second gate (orange) is a two-qbit gate, Controlled-NOT (CNOT), which flips Q_1 if and only if Q_0 is in the state $|1\rangle$. As a consequence, the consecutive two gates, Hadamard and CNOT, transform the two-qubits Q_0 and Q_1 into an entangled state$(|00\rangle + |11\rangle)/\sqrt{2}$, which finally leads to a GHZ or "cat" state$(|000\rangle + |111\rangle)/\sqrt{2}$, after the Toffoli gate.

This gate, when applied to a single spin initialized in its ground state $|0\rangle$, rotates the state vector by an angle of $\pi/2$ about the axis defined $z = x$, which creates a linear superposition of the two states ($|0\rangle$ and $|1\rangle$) of the qubit, $|+\rangle = (|0\rangle + |1\rangle)/\sqrt{2}$. If the qubit is initialized in its excited state $|1\rangle$, the Hadamard gate acts to create another superposition state of the qubit $|-\rangle = (|0\rangle - |1\rangle)/\sqrt{2}$, orthogonal to $|+\rangle$. The gate implemented in this way allows us to retrieve the behavior of the Hadamard gate on the selected states.

This set of two operations is very useful when creating an entanglement between two qubits as illustrated in the circuit example of Fig. 2(b). The Hadamard gate (H in the cyan box) acting on the first qubit Q_0 in its $|0\rangle$ state at t_0 transforms Q_0 into $|+\rangle$ state at t_1, which is going to influence the state of the second qubit Q_1 with the two-qubit gate Controlled-NOT (CNOT; orange) at t_1, leading to an entangled state of the two qubits $(|00\rangle + |11\rangle)/\sqrt{2}$ at t_2. A straightforward extension of this controlled operation to three-qubit system is the Controlled-controlled-NOT (CCNOT; Toffoli) gate, as depicted in purple. Together with the two qubits in the entangled state $(|00\rangle + |11\rangle)/\sqrt{2}$, the CCNOT gate includes the third qubit Q_2. The final circuit yields a fully entangled three-qubit state $(|000\rangle + |111\rangle)/\sqrt{2}$, the so-called Greenberger–Horne–Zeilinger (GHZ)[36] or cat state.

4.2. Two-qubit gate: controlled-NOT

To be universal, quantum control of multiple qubits only requires a reduced set of single-qubit gates and a two-qubit one. Among numerous two-qubit gates, the CNOT is a typical realization[37] in many available Noisy Intermediate-Scale Quantum (NISQ) architectures.[38] In reality, the CNOT gate can be implemented between two qubits with a minimal interaction obtained by placing them sufficiently far apart on the surface and in the presence of an Fe atom next to one of the Ti atoms. The effect of the Fe atom is to modify the nearby Ti atom allowing the addressability of each of the two qubits and to enhance the driving of the qubit even when the STM tip is away from it.[39,40] The weak interaction, in comparison with the detuning, permits to simplify the two-qubit state to products of the two single qubit states (Zeeman product states; $|00\rangle$, $|01\rangle$, $|10\rangle$, $|11\rangle$) with four available quantum transitions, as represented in the energy level diagram of Fig. 3(a). Similar to a single-qubit gate, in such a system we can drive a transition between any adjacent two-qubit states by tuning the RF frequency to the corresponding energy difference (f_1, f_2, f_3, or f_4).[39] In Fig. 3(b), a realization of a physical system of such two qubits using two Ti atoms on a 2 ML MgO surface is shown.[17]

A CNOT gate is a controlled operation where one of the qubits (the 'control' qubit) selects the action on the other qubit (the 'target' qubit). Thus, the NOT gate to the 'target' qubit only switches on, by flipping the target's initial state, when the 'control' qubit is exclusively in one of its two states, either $|0\rangle$ or $|1\rangle$. Here we choose the convention of flipping the second qubit when the first qubit is in the state $|0\rangle$. This is achieved by applying a π-pulse with an RF frequency corresponding to the energy of a specific transition in the two-qubit energy diagram (Fig. 3(a)). A π-pulse is an RF signal applied at the transition frequency for half a Rabi period, driving the system from one state of the transition to the other. Fig. 3(c) shows a result of Rabi oscillation measurement performed on the transition $|00\rangle \leftrightarrow |01\rangle$ of the two qubits in Fig. 3(b), with the experimental scheme of the pulsed double resonance ESR.[17] The flipping of one of the states corresponds to applying a Rabi oscillation by half of its period as indicated by the term 'π-time'. In practice, this inverses the state of the second (red) qubit if and only if the first (blue) qubit is in its $|0\rangle$ state. This RF pulse constitutes a CNOT gate where the 'control' qubit is the first and the 'target' qubit is the second qubit, Fig. 3.

4.3. Three-qubit gate: Toffoli gate

An experimental demonstration of a Toffoli (CCNOT) gate to a three-qubit system in ESR-STM has been realized by using three Ti atoms adsorbed onto a 2 ML MgO/Ag(100) surface (Fig. 4). See ref. 17 for the details of the physical system. Using the atom manipulation technique, the three atoms are precisely located in a specific environment, allowing for control over their mutual interactions and their coupling to the STM tip and external fields. As a result, the Zeeman product states of the

© 2025 The Author(s). Published by the Royal Society of Chemistry

Open Access Article. Published on 10 July 2025. Downloaded on 12/3/2025 1:48:05 AM.
This article is licensed under a Creative Commons Attribution 3.0 Unported Licence.

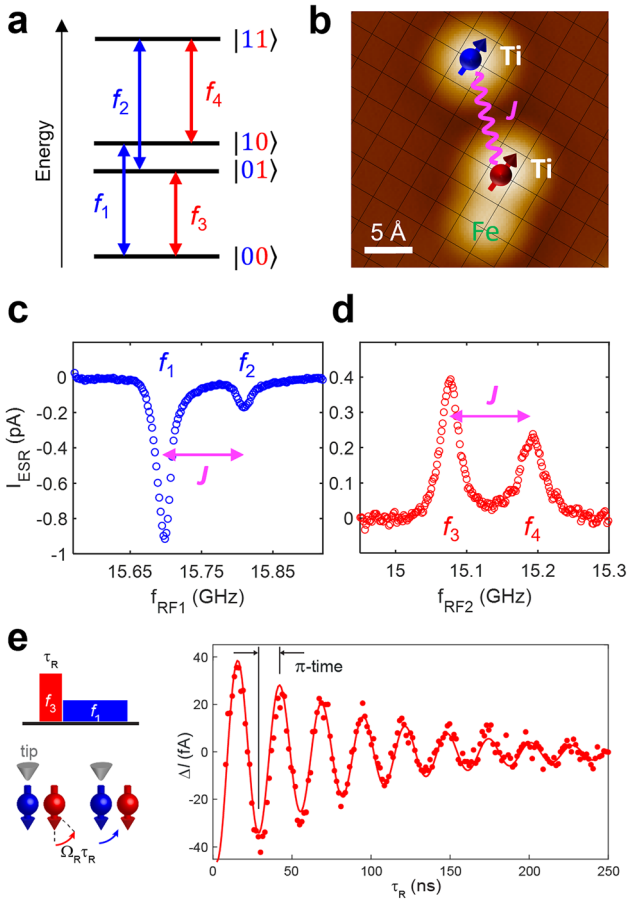


Fig. 3 (a) Energy diagram of a two-qubit system, illustrating its four eigenstates |00⟩, |01⟩, |10⟩, |11⟩ and four available quantum transitions represented by four corresponding frequencies f_1, f_2, f_3, f_4. (b) A two-qubit structure constructed using two Ti atoms, whose spins are weakly coupled (≈110 MHz) to each other, on a 2-monolayer-thick MgO surface. The "sensor" and "remote" qubits are depicted with blue and red colors. (c) and (d) ESR spectra measured by driving the blue Ti (f_1, f_2) and the red Ti (f_3, f_4) spins, respectively. (e) Schemes of RF pulses and responses of the two Ti spins for a controlled rotation of the "remote" qubit (left) and measured Rabi oscillations of the "remote" qubit, when the "sensor" qubit is in the state |0⟩ (right). This was achieved by a coherent driving of the transition f_3 (|00⟩ ↔ |01⟩) and subsequent steady-state probing using the transition f_1 (|00⟩ ↔ |10⟩) (see the scheme in (a)). The solid curve is a fit using an exponentially-decaying sinusoidal function. The duration of ≈13 ns for the CNOT operation is found as indicated by π-time.[17]

three qubits serve as good approximations to the eigenstates of the system, preserving the distinct energy levels necessary for the selective addressability of transitions corresponding to multi-qubit logic gates (Fig. 4(a)). RF pulses induce coherent Rabi oscillations between selected quantum states of the three-qubit system. By adjusting pulse amplitude, frequency, and duration, the system undergoes selective transitions corresponding to the logical action of the Toffoli gate.

A Toffoli gate is carried out by applying a sequence of RF pulses tuned to the transition frequencies between two eigenstates. In Fig. 4(b), a RF pulse scheme for Toffoli gate is illustrated for three qubits, composed of one "sensor" (blue) and two "remote" (red, purple) qubits. Here, the Toffoli gate involves flipping the state of the remote qubit 1 (RQ1; red) only when the other two qubits, sensor and remote qubit 2 (RQ2; purple), are in their |0⟩ states. This operation corresponds to the transition between |000⟩ and |010⟩.

Steady-state driving of four transitions (blue arrows in Fig. 4(a)) are used to probe the controlled rotation of RQ1, and resultant Rabi oscillation data are shown in Fig. 4(c). Coherent rotation of RQ1 appears only from the two probing transitions for RQ2 in the |0⟩ state (dark purple) while no oscillation is observed from the other two for RQ2 in the |1⟩ state (light purple). The Rabi frequencies associated with these transitions are sufficiently large to enable fast gate operations, with state transitions occurring on timescales as short as 20 ns. Such rapid operation times are advantageous, reducing exposure to decoherence and enhancing gate fidelity.

The successful demonstration of a Toffoli gate using ESR-STM highlights the potential for atomically precise spin systems to implement complex multi-qubit logic operations beyond single- and two-qubit gates as well as toward more sophisticated quantum operations necessary for fault-tolerant quantum computation. For instance, more complex quantum logic circuits can be realized using atomic spins on a surface, such as the one to create maximally entangled three-qubit states, *e.g.*, the GHZ state that was introduced in Fig. 2, by utilizing the experimental scheme shown in Fig. 4.

5. Implementation of multi-qubit control in an ESR-STM

Recent advances have demonstrated that ESR-STM is not limited to single-spin manipulation as introduced in the section II. It can be extended to the coherent control of multi-qubit systems assembled with atomic precision. However, it necessitates coherent control and measure of spins positioned outside the STM tunnel junction, the so-called "remote" qubits, which is implemented *via* an exchanged interaction with single-atom-magnets (here, Fe atoms; see Fig. 3(b)) that are judiciously placed a few MgO-lattice-constants apart and boost the driving of the ESR signal.[27] A recent experimental and theoretical studies show that the tip electric field modulates the interaction in time between the Fe and Ti atoms that serves as remote spin, leading to a strong coherent response of the Ti spin.[27,41] This approach effectively decouples the control and detection mechanisms of a spin, allowing for scalable multi-qubit architectures.

Initialization of the spins is achieved thermally by cooling the system to cryogenic temperatures (typically below 1 K) and applying an external magnetic field, resulting in most of the spin population in the ground-state. Detection of remote qubits is performed indirectly through the ESR transition of the "sensor" qubit, whose transition frequency depends on the quantum states of the coupled qubits. This transition frequency of the "sensor" qubit is carefully chosen by dipolar and exchange interactions with the "remote" qubit, which can be engineered through precise control over atomic separations of

© 2025 The Author(s). Published by the Royal Society of Chemistry

Open Access Article. Published on 10 July 2025. Downloaded on 12/3/2025 1:48:05 AM.
This article is licensed under a Creative Commons Attribution 3.0 Unported Licence.

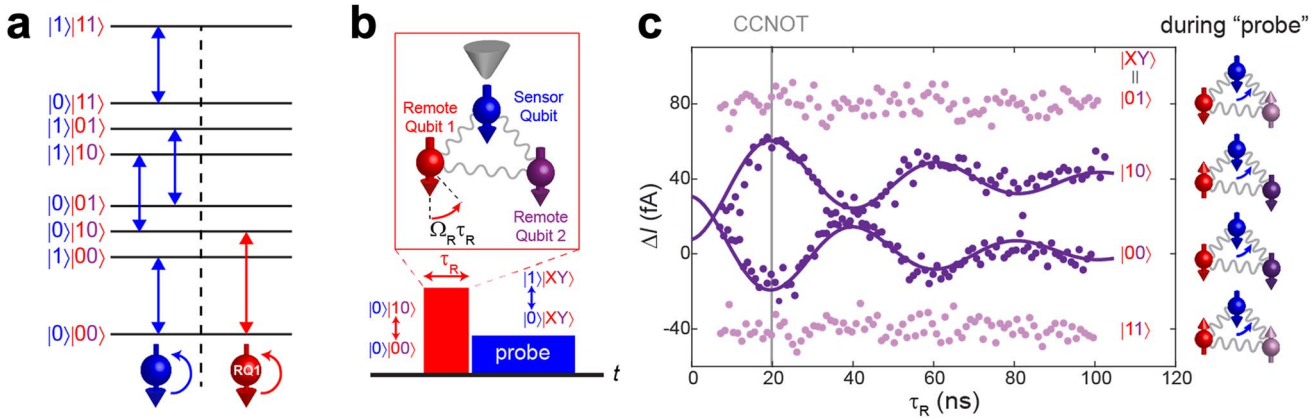


Fig. 4 (a) Energy diagram of the eight eigenstates of a three-qubit system, composed of one "sensor" (blue) and two "remote" (red, purple) qubits. (b) A scheme of pulsed double resonance ESR experiments performed on the three qubits (Ref. 17). During the measurement, the tip was parked only on the sensor qubit. The quantum transitions for driving the remote qubit 1 (RQ1; red) and for probing *via* the sensor qubit (blue) are depicted in (a). Spin arrow pointing down indicates ground state $|0\rangle$ of each qubit. (c) Pulsed double resonance data measured using the probe transitions indicated by the blue arrows in (a). Measurements using two probing transitions for RQ2 in the $|0\rangle$ ($|1\rangle$) state are indicated by dark (light) purple color. Note that this Toffoli gate is achieved just by about 20 ns.

the two qubits down to the sub-angstrom scale. Multiple remote qubits can be sensed simultaneously and their quantum states can be inferred from the distinct ESR transitions of the sensor qubit. An intriguing extension is to transpose this scheme to multi-magnetic-center molecules where different centers can be assigned to either the sensor or remote qubits, and can be manipulated to achieve multi-qubit quantum operations.[42]

5.1. Molecular qubits on a surface

Building these atomic-scale implementations on a solid surface, molecular qubits offer an opportunity to scale the ESR-STM approach to more complex and potentially more robust quantum systems. Molecular complexes can be chemically engineered to host multiple spin centers with tailored coupling strengths and coherence properties.[22,23] Fig. 5 illustrates how molecular arrays and molecular magnets can serve as platforms for implementing quantum logic operations. Fig. 5(a) shows molecular arrays on a surface that can be addressed individually with the ESR-STM. Fig. 5(b) shows a molecular magnet incorporating multiple spin centers, which demonstrates the potential for multi-qubit interactions. The recent experiments demonstrate that by driving an electron current through one of the active spins in a complex molecular system, other qubits within the molecule can be manipulated *via* a combination of inter-qubit coupling and time-dependent external fields.[24] Moreover, spectator spins, which are not directly addressed by the RF field, can act as mediators or enhancers of control signals, amplifying the reach of spin manipulation to more remote qubits within the system.[25]

The above strategy has already been applied to systems of weakly-coupled Ti spins on MgO surfaces. Extending these concepts to chemically designed molecular qubits holds a great

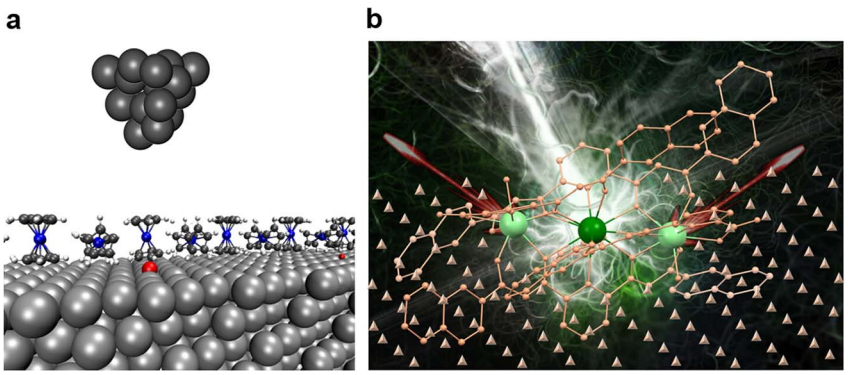


Fig. 5 (a) Schematic representation of molecular arrays on a surface, where individual molecules are engineered to address spin centers. These spin centers can be manipulated using Electron Spin Resonance Scanning Tunneling Microscopy (ESR-STM) to perform quantum logic gate operations. This approach enables precise control of quantum states at the atomic level. (b) Illustration of molecular magnets containing multiple spin centers, which can interact and potentially serve as multi-qubit systems (Adapted from ref. 44). These molecular architectures offer a promising platform for next-generation quantum computing applications due to their ability to maintain coherence and facilitate spin-based quantum information processing.

© 2025 The Author(s). Published by the Royal Society of Chemistry

Open Access Article. Published on 10 July 2025. Downloaded on 12/3/2025 1:48:05 AM. This article is licensed under a Creative Commons Attribution 3.0 Unported Licence.

promise for realizing universal quantum computation at the molecular level.[43] By using molecular self-assembly and precision chemistry, it becomes feasible to construct such systems systematically. Furthermore, the development of multi-qubit gates is of increasing interest due to their ability to reduce the depth of quantum circuits and to implement more efficient error mitigation schemes.[42] ESR-STM provides the necessary spatial and spectral resolution to implement these gates within molecular systems, offering a route toward scalable, high-density quantum processors.[44]

6. Conclusions

Electron spin resonance combined with scanning tunneling microscopy provides a unique and versatile platform for achieving quantum coherent manipulation of atomic and molecular qubits with unparalleled spatial and energy resolution. By combining the local addressability of STM with the spectral selectivity of ESR, ESR-STM offers precise control over individual spins, enabling universal set of quantum gates, composed of single-qubit rotations and CNOT. In this article, we have summarized the coherent manipulation of multi-qubit systems assembled on insulating surfaces with atomic precision, including the realization of Controlled-NOT and Toffoli gates. These achievements underscore the potential of ESR-STM for implementing complex quantum logic operations in atomically engineered qubit systems. Furthermore, by extending these techniques to chemically designed molecular qubits, ESR-STM opens new avenues for understanding single-qubit manipulations on the atomic and molecular scales, particularly exploring the extraordinary properties of molecules such as their inherent reproducibility, self-assembly, and tunability.

The successful demonstration of fast and coherent multi-qubit operations at the atomic scale represents an important step toward fault-tolerant quantum computation. The uniqueness of ESR-STM in engineering and addressing spin systems makes it a valuable tool not only for fundamental studies of quantum coherence and entanglement but also for the practical development of high-density quantum processors. Future work will focus on increasing the complexity of qubit architectures, improving coherence times, and integrating molecular qubit networks to advance scalable quantum information processing.

Data availability

Fig. 1 data for this article are available at DOI: **https://doi.org/10.1126/science.aay6779**. Fig. 3 data for this article are available at DOI: **https://doi.org/10.1126/science.ade5050**. Fig. 4 data for this article are available at DOI: **https://doi.org/10.1126/science.ade5050**. Fig. 5(b) data for this article are available at **https://doi.org/10.1021/acs.inorgchem.2c03940**.

Conflicts of interest

There are no conflicts to declare.

Acknowledgements

We thank projects PID2021-127917NB-I00 by MCIN/AEI/10.13039/501100011033, QUAN-000021-01 by Gipuzkoa Provincial Council, PIBA-2024-1-0008 and IT-1527-22 by Basque Government, ESiM project 101046364 by EU. Views and opinions expressed are however those of the author(s) only and do not necessarily reflect those of the EU. Neither the EU nor the granting authority can be held responsible for them. SP and AJH acknowledge supports from Institute for Basic Science (grant: IBS-R027-D1).

References

1 J. Preskill, *Quantum*, 2018, **2**, 79.
2 M. Kjaergaard, M. E. Schwartz, J. Braumüller, P. Krantz, J. I. J. Wang, S. Gustavsson and W. D. Oliver, *Annu. Rev. Condens. Matter Phys.*, 2020, **11**, 369.
3 L. Henriet, L. Beguin, A. Signoles, T. Lahaye, A. Browaeys, C. Jurczak, G. Reymond and J. Esteve, *Quantum*, 2020, **4**, 332.
4 M. Veldhorst, *et al.*, *Nat. Commun.*, 2017, **8**, 1766.
5 E. Charbon *et al.*, in *2021 IEEE International Solid-State Circuits Conference (ISSCC)*, 2021, pp. 304–306.
6 C. P. Poole Jr, *Electron Spin Resonance: A Comprehensive Treatise on Experimental Techniques*, 2nd edn, Dover Publications, 1996.
7 R. Wiesendanger, *Scanning Probe Microscopy and Spectroscopy: Methods and Applications*, Cambridge University Press, 1994.
8 S. Baumann, W. Paul, T. Choi, C. P. Lutz, A. Ardavan and A. J. Heinrich, *Science*, 2015, **350**, 417.
9 T. Choi, W. Paul, S. Rolf-Pissarczyk, A. J. MacDonald, F. D. Natterer, K. Yang, P. Willke, C. P. Lutz and A. J. Heinrich, *Nat. Nanotechnol.*, 2017, **12**, 420.
10 P. Willke, Y. Bae, K. Yang, J. L. Lado, A. Ferrón, T. Choi, A. Ardavan, J. Fernández-Rossier, A. J. Heinrich and C. P. Lutz, *Science*, 2018, **362**, 336.
11 T. S. Seifert, S. Kovarik, D. M. Juraschek, N. A. Spaldin, P. Gambardella and S. Stepanow, *Sci. Adv.*, 2020, **6**, eabc5511.
12 X. Zhang, C. Wolf, Y. Wang, H. Aubin, T. Bilgeri, P. Willke, A. J. Heinrich and T. Choi, *Nat. Chem.*, 2022, **14**, 59.
13 S. Kovarik, R. Robles, R. Schlitz, T. S. Seifert, N. Lorente, P. Gambardella and S. Stepanow, *Nano Lett.*, 2022, **22**, 4176.
14 A. J. Heinrich, W. D. Oliver, L. M. K. Vandersypen, A. Ardavan, R. Sessoli, D. Loss, A. B. Jayich, J. Fernandez-Rossier, A. Laucht and A. Morello, *Nat. Nanotechnol.*, 2021, **16**, 1318.
15 K. Yang, W. Paul, S.-h. Phark, Y. J. Bae, R. Melghem, S. Rolf-Pissarczyk and A. J. Heinrich, *Science*, 2019, **366**, 509.
16 L. M. Veldman, L. Farinacci, R. Rejali, R. Broekhoven, J. Gobeil, D. Coffey, M. Ternes and A. F. Otte, *Science*, 2021, **372**, 964.
17 Y. Wang, Y. Chen, H. T. Bui, C. Wolf, M. Haze, C. Mier, J. Kim, D. J. Choi, C. P. Lutz, Y. Bae, S. H. Phark and A. J. Heinrich, *Science*, 2023, **382**, 87.
18 B. M. Terhal, *Rev. Mod. Phys.*, 2015, **87**, 307.

© 2025 The Author(s). Published by the Royal Society of Chemistry

Open Access Article. Published on 10 July 2025. Downloaded on 12/3/2025 1:48:05 AM.
This article is licensed under a Creative Commons Attribution 3.0 Unported Licence.

19 E. T. Campbell, B. M. Terhal and C. Vuillot, *Nature*, 2017, **549**, 172.
20 M. Atzori and R. Sessoli, *J. Am. Chem. Soc.*, 2019, **141**, 11339.
21 M. N. Leuenberger and D. Loss, *Nature*, 2001, **410**, 789.
22 A. Cornia, M. Affronte, D. Gatteschi, R. Sessoli, M. Mannini, E. Coronado, F. Luis, M. Malavolti, P. Santini and S. Carretta, *Nat. Rev. Chem.*, 2020, **4**, 71.
23 M. Warner, S. Din, I. S. Tupitsyn, G. W. Morley, A. M. Stoneham, J. A. Gardener, Z. Wu, A. J. Fisher, S. Heutz, C. W. M. Kay and G. Aeppli, *Nature*, 2013, **503**, 504.
24 M. Morgado, S. Whitlock, Quantum simulation and computing with Rydberg-interacting qubits, *arXiv*, 2020, preprint, arXiv:2011.03031v2, DOI: **10.48550/arXiv.2011.03031**.
25 A. Ardavan, O. Rival, J. J. L. Morton, S. J. Blundell, A. M. Tyryshkin, G. A. Timco and R. E. P. Winpenny, *Phys. Rev. Lett.*, 2007, **98**, 057201.
26 S. Hill, *Phys. Today*, 2025, **78**, 38.
27 S.-h. Phark, H. T. Bui, A. Ferrón, J. Fernández-Rossier, J. Reina-Gálvez, C. Wolf, Y. Wang, K. Yang, A. J. Heinrich and C. P. Lutz, *Adv. Sci.*, 2023, **10**, 2302033.
28 Y. Wang, M. Haze, H. T. Bui, W.-h. Soe, H. Aubin, A. Ardavan, A. J. Heinrich and S.-h. Phark, *Npj Quantum Inf.*, 2023, **9**, 1.
29 J. L. Lado, A. Ferrón and J. Fernández-Rossier, *Phys. Rev. B*, 2017, **96**, 205420.
30 J. Reina Gálvez, C. Wolf, F. Delgado and N. Lorente, *Phys. Rev. B*, 2019, **100**, 035411.
31 S. Kovarik, R. Schlitz, A. Vishwakarma, D. Ruckert, P. Gambardella and S. Stepanow, *Science*, 2024, **384**, 1368.
32 R. Kawaguchi, K. Hashimoto, T. Kakudate, K. Katoh, M. Yamashita and T. Komeda, *Nano Lett.*, 2023, **23**, 123.
33 S.-h. Phark, J. A. Fischer, M. Corbetta, D. Sander and J. Kirschner, *Appl. Phys. Lett.*, 2013, **103**, 032407.
34 S. H. Phark, J. A. Fischer, M. Corbetta, D. Sander, K. Nakamura and J. Kirschner, *Nat. Commun.*, 2014, **5**, 5183.
35 S.-h. Phark and D. Sander, *Nano Convergence*, 2017, **4**, 8.
36 D. M. Greenberger, M. A. Horne, A. Shimony and A. Zeilinger, *Am. J. Phys.*, 1990, **58**, 1131.
37 M. A. Nielsen and I. L. Chuang, *Quantum Computation and Quantum Information*, Cambridge University Press, 2000.
38 A. Javadi-Abhari, M. Treinish, K. Krsulich, C. J. Wood, J. Lishman, J. Gacon, S. Martiel, P. D. Nation, L. S. Bishop, A. W. Cross, B. R. Johnson and J. M. Gambetta, Quantum computing with Qiskit, *arXiv*, 2024, preprint, arXiv:2405.08810v3, DOI: **10.48550/arXiv.2405.08810**.
39 S. H. Phark, Y. Chen, H. T. Bui, Y. Wang, M. Haze, J. Kim, Y. Bae, A. J. Heinrich and C. Wolf, *ACS Nano*, 2023, **17**, 14144.
40 H. T. Bui, C. Wolf, Y. Wang, M. Haze, A. Ardavan, A. J. Heinrich and S.-h. Phark, *ACS Nano*, 2024, **18**, 12187.
41 J. Reina-Gálvez, H.-A. Le, H. T. Bui, S.-h. Phark, N. Lorente, and C. Wolf, Efficient driving of a spin-qubit using single-atom magnets, *arXiv*, 2024, preprint, arXiv:2408.07289v2, DOI: **10.48550/arXiv.2408.07289**.
42 I. Borilovic, O. Roubeau, B. L. Guennic, J. van Slageren, S. Lenz, S. J. Teat and G. Aromí, *Chem. Commun.*, 2022, **58**, 7530.
43 L. A. Barrios, D. Aguilà, O. Roubeau, P. Gamez, J. Ribas-Ariño, S. J. Teat and G. Aromí, *Chem. - Eur. J.*, 2009, **15**, 11235.
44 D. Maniaki, A. Sickinger, L. A. Barrios Moreno, D. Aguilà, O. Roubeau, N. S. Settineri, Y. Guyot, F. Riobé, O. Maury, L. A. Galán and G. Aromí, *Inorg. Chem.*, 2023, **62**, 3106.

© 2025 The Author(s). Published by the Royal Society of Chemistry